Intranasal lipid nanocarriers: Uptake studies with fluorescently labeled formulations

Intranasal lipid nanocarriers: uptake studies with fluorescently labelled formulations

Elisabetta Muntoni [a], Elisabetta Marini [a], Chiara Ferraris [a], Sara Garelli [a], Maria Teresa Capucchio [b], Elena Colombino [b], Pier Paolo Panciani [c], Luigi Battaglia [a]*

[a] *Department of Drug Science and Technology, University of Turin, via Pietro Giuria 9, 10125 Turin, Italy; elisabetta.muntoni@unito.it; elisabetta.marini@unito.it; chiara.ferraris@unito.it; sara.garelli@unito.it*

[b] *Department of Veterinary Sciences, University of Turin, Largo Paolo Braccini 2, 10195 Grugliasco, Turin, Italy; mariateresa.capucchio@unito.it; elena.colombino@unito.it*

[c] *Spedali Civili, Section of Neurosurgery, Piazzale Spedali Civili 1, 25123 Brescia, Italy; pierpaolo.panciani@gmail.com*

*Email: luigi.battaglia@unito.it; Phone: +39-011-670-7142

ABSTRACT: Drug delivery by the intranasal route allows both systemic absorption and non-invasive brain targeting, due to the unique connection provided by the olfactory and trigeminal nerves between the brain and the external environment. Lipid nanocarriers can improve intranasal drug delivery by enhancing bioadhesion to nasal mucosa, and by protecting the encapsulated drug from biological degradation and transport efflux proteins. In this study two different biocompatible lipid nanocarriers were compared: nanoemulsions and solid lipid nanoparticles. The nasal uptake was investigated by labelling the nanocarriers lipid matrix with two fluorescent probes, 6-coumarin and rhodamine B, both lipophilic, yet characterized by different water solubility, in order to mimic the behaviour of hypothetic drug compounds. *Ex vivo* permeation, *in vivo* pharmacokinetics and biodistribution studies were performed. 6-coumarin, water insoluble and therefore integral with the lipid matrix, was taken up to a limited extent, within a long timeframe, but with a proportionally more pronounced brain accumulation. In nanoemulsions soluble rhodamine B showed a relevant systemic uptake, with good bioavailability, likely due to the prompt release of the probe at the nasal mucosa.

KEYWORDS: *nanoemulsions, solid lipid nanoparticles, intranasal delivery, 6-coumarin, rhodamine B*

INTRODUCTION

Drug delivery by the intranasal (i.n.) route allows both systemic absorption and non-invasive brain targeting, by overcoming the blood-brain barrier (BBB). Indeed, following i.n. administration, drugs are exposed to the nasal mucosa, which is innervated by olfactory and trigeminal nerves, allowing nose-to-brain uptake [1, 2]. The intra-neuronal route exploits the termination of olfactory bulb and trigeminal nerve protruding in the mucosa, while the paracellular way occurs through the extracellular clefts between the mucosal cells and the neurons. The former involves the axonal transport of lipid soluble molecules, is size limited (<700 nm) and requires a long time (few hours) to reach the different brain regions. The latter is associated with rapid delivery (almost immediately after intranasal administration) and simultaneous systemic absorption in the bloodstream: indeed, after reaching the lamina propria through the extracellular space, substances can shift towards the cranial compartment or the general systemic circulation [3, 4]. This route is associated with tight junctions, intracellular space, gaps, or pores present between the epithelial cells, and constitutes an important pathway for the absorption of small molecular weight (MW) (less than 1000 Da), polar or hydrophilic compounds, but it is less selective for the brain, with respect to the intra-axonal pathway [2]. Systemic absorption within the bloodstream through the highly vascularized lamina propria can be achieved also by transcellular route through the epithelial cells of the nasal mucosa [5].

I.n. delivery shows several advantages over other administration routes, including fast onset of action, avoidance of the intestinal and hepatic pre-systemic disposition, reduction of systemic exposure and side effects, direct delivery and targeting to the brain, ease of administration and better patient compliance. Major drawbacks are the muco-ciliary clearance of nasally applied drugs, the low permeability for high MW drugs, the enzymatic degradation by nasal cytochrome P450/peptidases/proteases, the limitation to potent drugs or small volumes administered, and the influence of nasal irritation on drug absorption [6, 7]. To this aim several promoters for nasal uptake have been proposed, some of them being already marketed for the systemic delivery of small MW drugs or peptides, especially where a rapid onset of action is required [8, 9]. Within this concern, also nanocarriers have been investigated, since they can enhance bioadhesion to nasal mucosa and protect the encapsulated drug from biological degradation and transport efflux proteins [10]. Indeed, particulate uptake, while of relatively low efficiency, also occurs in the nasal mucosa [11]. Nanoparticles with hydrophilic surface may exploit the paracellular route, but with a size cut-off of 50 nm, whereas hydrophobic ones are mainly transported via the intracellular pathway, which is only size limited by the average diameter of olfactory axons. [12]. Lipid colloidal systems are classical prototypes proposed for intranasal delivery. Among them, vescicles, such as liposomes, showed tendency to increase the brain uptake of encapsulated drugs, regardless of their size, but owing to their flexibility, which can be further enhanced by using edge activators [12]. Nonetheless, some stability issues and technological problems (including batch to batch reproducibility, shortage of feasible sterilization methods, low drug entrapment, poor particle size control, difficult production of large batch sizes) affect liposomes manufacturing [13]. On the contrary, lipid-based nanocarriers, such as solid lipid nanoparticles (SLN) and nanoemulsions, have relevant technological advantages over liposomal formulations for intranasal administration. Indeed, they are composed either by biocompatible solid lipid or oily core, stabilized by surfactants: the lipid component favours the bioadhesion to the olfactory epithelium and the partition of the nanoparticles/nanodroplets in the nasal mucosa, and the surfactant enhances the penetration of biological membranes. Moreover, they can be manufactured at low cost, owing to solvent-free and easy to scale-up methods, they are able to encapsulate poorly water soluble drugs with an high payload and show good physical-chemical stability, allowing the possibility of steam sterilization. Therefore, relevant research is currently focused on SLN and nanoemulsions for intranasal administration [14, 15]. However, despite the emerging literature in the field, the actual relevance of such lipid-based nanocarriers as nasal devices is still controversial. Within this concern, a systematic comparison among various lipid matrixes, as well as between free and encapsulated drugs, and between i.n. and systemic administration routes should be carefully investigated.

In this experimental study, a prototype for each of the two above-mentioned biocompatible lipid-based nanocarriers were compared after i.n. administration. SLN, obtained by coacervation, were stabilized by bioadhesive polymers (increasing nasal retention). Commercial nanoemulsions, usually employed for parenteral nutrition, instead, were functionalized with two alternative nasal permeation enhancers: biliary

salts (acting through tight junction opening and ciliary inhibition) and thickeners (increasing nasal retention) [16]. In order to mimic the behavior of hypothetic drug compounds, such formulations were labelled with two fluorescent probes, both lipophilic, yet characterized by different water solubility. The water insoluble probe 6-coumarin (6-cou) allowed to label both the nanocarriers, being integral with the lipid matrix [17, 18]. Rhodamine B (rod-B), being slightly water-soluble, although lipophilic, was used to label the nanoemulsions, owing to partition into its oily phase. A multi-step investigation approach was followed: *ex vivo* permeation on excised bovine turbinates, *in vivo* pharmacokinetics and biodistribution in healthy male Wistar rats were performed. In each set of experiments labelled formulations were compared with free probes. Moreover, biodistribution after i.n. and intravenous (i.v.) administration of the formulations under study were compared.

MATERIALS AND METHODS

Chemicals. 1-heptanesulfonic acid sodium salt, 6-cou, 60000-90000 MW dextran, dimethyl sulfoxide (DMSO), ethanol, sodium glycodeoxycholate (GDC), 85000-120000 MW 99% hydrolyzed polyvinyl alcohol (PVA 85000), 9000-10000 MW 80% hydrolyzed polyvinyl alcohol (PVA 9000), rod-B were from Sigma-Aldrich (St. Louis, MO, USA). Ammonium chloride, sodium chloride and sodium hydroxide are from Carlo Erba Reagents S.r.l. (Cornaredo, Italy). Methanol, hydrochloric acid were from Merck (Darmstadt, Germany). Sodium behenate was from Nu-Chek Prep (Eleysian, MN, USA). Isoflurane was from Alcyon (Cherasco, Italy). 10% Intralipid® (IL) was from Fresenius Kabi (Bad Homberg, Germany). Kolliphor® EL was a kind gift from BASF (Ludwigshafen, Germany). Distilled water was purified using a MilliQ system (Millipore, Bedford, MO, USA). All other chemicals were of analytical grade and used without further purification.

Tissues. Nasal permeation was studied using bovine nasal mucosa. Bovine nasal mucosa was obtained from animals regularly slaughtered at the teaching slaughterhouse of the Department of Veterinary Sciences, University of Turin, within two hours from death. Animal nasal mucosa (except the septum part) was excised and separated from the superior nasal concha by two animal pathologists. Tissues were stored in phosphate buffer saline (PBS), pH 6.4, until further analysis. Nasal mucosa was also assessed by hematoxylin & eosin (H&E) staining (Figure S1) in order to confirm that standard slaughter procedure and sampling did not affect the tissue integrity.

Animals. Male Wistar rats (Charles River, MA, USA), weighing 250 g, were housed in standard facilities, handled and maintained according to our Institutional Animal Care and Use Committee ethical regulations. Rats were kept under controlled environmental conditions (24 ± 1 °C, 50–60% humidity, 12 h light and dark cycles, lights on at 7:00 am). Rats were given ad libitum access to food and water. The procedures conformed to the Ethics Committee of University of Turin's institutional guidelines on animal welfare (DL 26/2014 implementation of directive 2010/63 UE) as well as International Guidelines, and all efforts were done to minimize the number of animals and their discomfort. All experiments on animal models were performed according to an experimental protocol approved by the University Bioethical Committee and the Italian Ministry of Health (Aut. N. 814/2018-PR).

Formulations. Commercial IL was used as the nanoemulsion. IL was also functionalized with GDC, a biliary salt (5 mg/mL): GDC was added directly to IL under vortex, followed by ultrasound treatment for one minute (ELMA, Transsonic 660/H). PVA 85000 was dissolved at 10% in water under steam and used as thickener for IL for an alternative functionalization (IL PVA). Fluorescent probes were pre-dissolved in DMSO and added to IL formulations under vortex.

Behenic acid SLN were prepared by the fatty acid coacervation method [19-21]. Briefly, sodium behenate was dispersed in water with PVA 9000 and the mixture was then heated under stirring (300 rpm), to obtain a clear micellar solution. Ammonium chloride, followed by hydrochloric acid, wasused as the coacervating solution; they were added dropwise to the mixture until complete behenic acid precipitation.

The obtained suspension was then cooled under stirring at 300 rpm until 15°C temperature was reached. 6-cou, pre-dissolved in DMSO, was added to the sodium behenate micellar solution prior to acidification.

Free fluorescent probes, used as controls, were prepared as follows: rod-B was dissolved in normal saline; 6-cou solution was obtained in Kolliphor® EL/ethanol mixture and diluted in normal saline; a gross 6-cou suspension was formulated in normal saline.

Characterization of Labelled Lipid Nanocarriers. Mean particle sizes (intended as hydrodynamic diameter), polydispersity and Zeta potential of lipid nanocarriers were determined 1 h after preparation using the dynamic light scattering technique (DLS; 90 Plus, Brookhaven, NY, USA). Size measurements were obtained at an angle of 90° and Zeta potential at an angle of 15°, both at a temperature of 25°C. The homogeneity of the suspension was checked with optical microscopy (DM2500, Leica Microsystems, Wetzlar, Germany). Fluorescent probe % recovery and % entrapment efficiency (EE%) were determined as follows: 0.1 mL of labelled SLN suspension was diluted with 0.1 mL water, while 0.1 mL of labelled IL nanoemulsion was diluted with 0.1 mL 60000-90000 MW dextran 30% water solution. Both were centrifuged for 15 min at 62000 g (Allegra® 64R centrifuge, Beckmann Coulter, Palo Alto, CA, USA). The supernatant (unentrapped probe) was diluted in 0.8 mL methanol and centrifuged. The entrapped probe was extracted from the lipid pellet with 0.8 mL methanol, following dilution in 0.2 mL water and centrifugation, in order to discard the precipitated lipids. Obtained samples were analyzed spectrophotometrically (6-cou: λ=450 nm; rod-B: λ= 550 nm). Fluorescent probe % recovery was calculated as the ratio between the total amount of probe in the supernatant and in the pellet vs the total weighted, while the EE% as the ratio between the amount of probe in the pellet vs the total amount in the supernatant and in the pellet.

Release Studies. Release of fluorescent probes from IL was assessed through the dialysis bag method. Three mL of labelled IL were put in the bag and dialyzed vs 100 mL distilled water under stirring. At scheduled times the receiving phase was analyzed spectrophotometrically (6-cou: λ=450 nm; rod-B: λ= 550 nm).

***Ex Vivo* Permeation Studies.** The permeation and accumulation in the nasal mucosa were studied by using the Sartorius Absorption Simulator (Gottingen, Germany). One mL of labelled formulations was put in contact with the mucosa (2.32 cm^2); the receiving phase was constituted by 20 mL of Krebs–Ringer buffer (KRB), kept at 37°C. At scheduled times, 0.5 mL of the receiving phase were withdrawn and replaced with KRB. Quantification of the permeated probe was performed through spectrofluorimetry by using a Multilabel Plate Reader (Victor^3 1420, Perkin Elmer, Waltham, MA, USA): 6-cou λ_{exc}=450 nm, λ_{em}=490; rod-B λ_{exc}=485 nm, λ_{em}=540. At the end of the experiment, the mucosa was washed with normal saline; drug accumulation in the tissue was determined through a High Pressure Liquid Chromatography (HPLC) analysis after extraction with 2 mL of a 75:25 methanol/water mixture , as described below. Tests were carried out in duplicate for each formulation under study.

Pharmacokinetics after i.n. Administration. One hundred μL of the labelled formulations under study (50 μL for each nostril) were administered to rats during a 10 min timeframe with the aid of a pipette tip, by keeping animals under isoflurane anesthesia. At scheduled times after formulations administration, blood samples were collected through a catheter surgically positioned in the rat jugular vein. Blood samples were centrifuged to isolate plasma. Plasma concentration of the fluorescent probes was determined after deproteinization (100 μL of plasma diluted with 300 μL methanol and centrifuged) by means of HPLC, as described below. In the case of 6-cou labelled formulations, samples were concentrated 10-folds under nitrogen steam before injection to HPLC. Tests were carried out in duplicate for each formulation under study.

Biodistribution after i.n. Administration. Administration of labelled formulations was performed as in the pharmacokinetic study. After animal sacrifice performed at scheduled times, plasma was withdrawn and the organs (liver, spleen, kidneys, lungs, heart and brain) were removed surgically. Blood samples were collected in heparinized tubes and centrifuged to isolate plasma. The brain underwent capillary depletion to

isolate brain capillaries from parenchyma. Briefly, freshly removed brains were manually homogenized with a potter in 3.5 mL Phosphate Buffered Saline (PBS) buffer; then, 1 mL of the homogenate was diluted with 1.16 mL dextran 60000–90000 and underwent gradient centrifugation at 4000 g for 10 min at 25°C in a test tube (Allegra® 64R centrifuge, Beckmann Coulter, Palo Alto, CA, USA). The capillaries were isolated from the bottom of the tube [22]. Other organs were homogenized with UltraTurrax® (IKA, Staufen, Germany) for 5 min in water at a tissue concentration of 125 mg/mL. Tissue homogenates and plasma underwent deproteinization (100 μL of sample diluted with 300 μL methanol and centrifuged) prior to HPLC analyses, as described below. In the case of 6-cou labelled formulations, samples were concentrated 10-folds under nitrogen steam before injection to HPLC. Experiments were performed in duplicate for each experimental condition.

Biodistribution after i.v. Administration. One hundred μL of the labelled formulations under study were administered to rats by injection in the lateral tail vein. Animals were sacrificed 1 h after administration. Plasma and organs underwent the same procedures of i.n. biodistribution, but no concentration of 6-cou samples was necessary. Tests were carried out in duplicate for each formulation under study.

HPLC Analyses. Analyses were performed with a Jasco PU-1585 pump, equipped with a Shimadzu RF-551 fluorescence detector (Shimadzu, Tokyo, Japan), linked to a CromatoPlus software for data analysis (Aqualis srl, Nerviano, Italy).

6-cou: column was a Chromsystem RP18 12.5x0.46cm (Gräfelfing, Germany). Eluent was 0.1% 1-heptanesulfonate 40%, acetonitrile 60%. Flow rate was set at 1 mL/min. Fluorimeter was set at λ_{exc}=450 nm and λ_{em}=490 nm. Retention time was 4.0 min [23].

Rod-B: column was a C18 Mediterranea Sea 5 μm 15x0.46 (Teknocroma, Barcelona, Spain). Eluent was 80% methanol. Flow rate was set at 1 mL/min. Fluorimeter was set at λ_{exc}=550 nm and λ_{em}=590 nm. Retention time was 5.0 min.

Statistical Analysis. Results were reported as mean ± SEM, and statistical analysis was performed using a two-tailed Student's t-test (Prism Graphpad 7.0, Graphpad Software, San Diego, CA, USA, 2016), in order to compare every single formulation *vs* free probe.

RESULTS

IL was functionalized with GDC for its ciliary inhibition ability and capacity of tight junctions opening, and, alternatively, with PVA 85000 as a thickener to increase nasal retention [16]. Behenic acid SLN were obtained by fatty acid coacervation method, using bioadhesive PVA 9000 as the suspending agent [19-21]. Free probes solutions were used as controls. To this aim, different free 6-cou formulations were employed for i.n. and i.v. administration respectively, owing to 6-cou negligible water solubility. Indeed, 6-cou was dissolved in Kolliphor® EL/ethanol mixture and diluted in normal saline for i.v. administration. On the contrary, a gross 6-cou suspension in normal saline was nasally administered, in order to avoid the permeation enhancement due to the excipients. Composition and physico-chemical characterization of labelled nanocarriers is shown in Table 1. Noteworthy, while IL is stabilized by the negative Zeta potential of lecithin emulsifier, SLN showed no surface charge, since they are sterically stabilized by neutral polymer PVA 9000. Loading of fluorescent probes has slight influence on the particle size. Noteworthy, the size of fluorescent probe loaded IL GDC increases from 248 nm to 332 nm upon switching from 6-cou to rod-B, probably because an electrostatic interaction occurs between rod-B and GDC. Indeed, unlike 6-cou, rod-B is a quaternary ammonium salt, whose positive charge may interact with the negative charge of GDC carboxylate, leading to a slight increase in particle size. EE% was higher than 85% for both the fluorescent probes in IL, as well as for 6-cou in SLN, meaning that the unbound amount was negligible for our purposes. Therefore, no purification step either from unbound labels or from DMSO, used to solubilize the fluorescent probes, was needed for the subsequent experiments. Indeed, with regard to animal models, the total amount of co-solvent administered was below the maximum volume allowed in rodents (0.1 mL/kg of DMSO 100%

w/w) for intravenous injection. Moreover, DMSO concentration in the same formulations was below the co-solvents limit (25%) for intravenous formulations [24].

Table 1. Composition and physico-chemical characterization of labelled blank formulations

	SLN		IL			IL PVA			IL GDC			6-cou solution	6-cou suspension	rod-B solution
Sodium behenate (mg)	25.00		—			—			—			—	—	—
Sodium hydroxide 1M (μL)	30.00		—			—			—			—	—	—
IL (mL)	—		5.00			5.00			5.00			5.00	—	—
PVA 9000 (mg)	50.00		—			—			—			—	—	—
PVA 85000 10% (mL)	—		—			1.25			—			—	—	—
GDC (mg)	—		—			—			25.00			—	—	—
Ammonium chloride 5M (μL)	65.00		—			—			—			—	—	—
Hydrochloric acid 1M (μL)	100.00		—			—			—			—	—	—
Distilled water (mL)	2.50		—			—			—			—	—	—
Normal saline (mL)	—		—			—			—			0.50	1.00	1.00
Kolliphor® EL (μL)	—		—			—			—			250.00	—	—
Ethanol (μL)	—		—			—			—			250.00	—	—
	6-cou labelled	**Blank**	**6-cou labelled**	**rod-B labelled**	**Blank**	**6-cou labelled**	**rod-B labelled**	**Blank**	**6-cou labelled**	**rod-B labelled**	**Blank**			
5 mg/mL 6-cou DMSO solution (μL)	25.00	—	100.00	—	—	100.00	—	—	100.00	—	—	20.00	20.00	—
5 mg/mL rod-B DMSO solution (μL)	—	—	—	100.00	—	—	100.00	—	—	100.00	—	—	—	20.00
Mean size (nm)	248.6	243.2	249.1	245.7	247.9	343.9	317.0	295.6	247.9	332.0	276.4	—	—	—
Polydispersity	0.090	0.084	0.163	0.154	0.088	0.216	0.168	0.131	0.039	0.103	0.025	—	—	—
Z Potential (mV)	N.D.	N.D.	-36.45	-37.57	-39.72	-40.52	-30.67	-30.34	-39.92	-39.53	-36.96	—	—	—
Recovery %	82%	—	73%	69%	—	N.D.	N.D.	—	N.D.	N.D.	—	—	—	—
EE %	98%	—	92%	85%	—	N.D.	N.D.	—	N.D.	N.D.	—	—	—	—

Abbreviations: 6-cou: 6-coumarin; DMSO: dimethyl sulfoxide; EE %: % entrapment efficiency; GDC: sodium glycodeoxycholate; IL: 10% Intralipid®; PVA 85000: 85000-120000 MW 99% hydrolyzed polyvinyl alcohol; PVA 9000: 9000-10000 MW 80% hydrolyzed polyvinyl alcohol; rod-B: rhodamine B; SLN: solid lipid nanoparticles.

Release of the two fluorescent probes from IL to normal saline is shown in Figure 1: since 6-cou is water insoluble, release is modest and 6-cou is integral with the lipid matrix. Instead, in the case of rod-B, prompt release is obtained due to its slight water solubility.

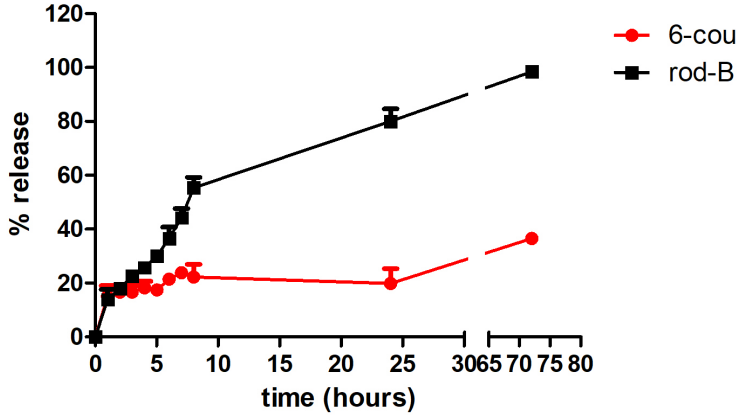

Figure 1. Release of fluorescent probes from labelled 10% Intralipid® (IL). Abbreviations: 6-cou: 6-coumarin; rod-B: rhodamine B.

Relevant differences were also noticed between the *ex vivo* permeation of the two fluorescent probes through bovine nasal mucosa (Figure 2). Indeed, while relevant permeation was measured for rod-B loaded formulations, 6-cou permeation was undetectable. A nearly 100-folds higher accumulation in mucosal tissue was revealed for rod-B compared to 6-cou. Furthermore, the mean permeation of rod-B decreased when loaded in IL. Selected enhancers did not cause a statistically significant increase of rod-B permeation from IL, despite IL GDC mean permeation profile was superior to those of IL and IL PVA.

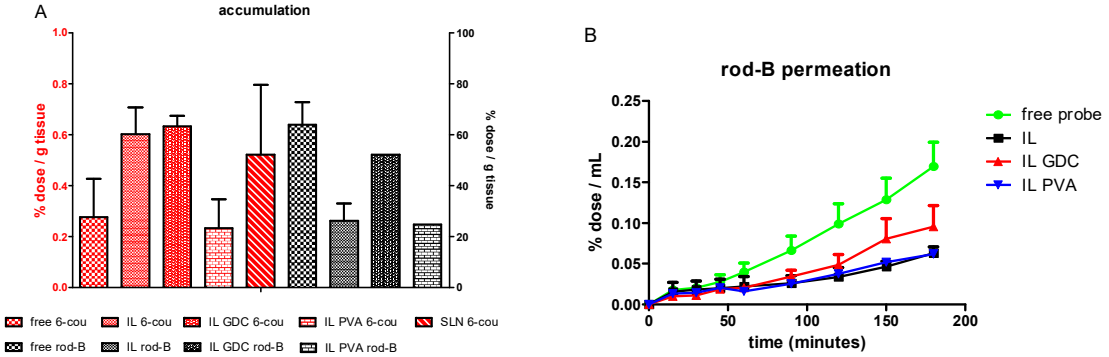

Figure 2. Accumulation (A) and permeation (B) of labelled formulations across bovine nasal mucosa. Abbreviations: 6-cou: 6-coumarin; IL: 10% Intralipid®; IL GDC: sodium glycodeoxycholate functionalized IL; IL PVA: 85000-120000 MW 99% hydrolyzed polyvinyl alcohol functionalized IL; rod-B: rhodamine B; SLN: solid lipid nanoparticles.

Consistently, in pharmacokinetic experiments after i.n. administration rod-B uptake was nearly 100-folds higher compared to 6-cou. Moreover, rod-B uptake was rapid, with a similar profile among all the formulations under study. In agreement with permeation studies, IL decreased systemic absorption compared to free probe, and, despite the mean pharmacokinetic profile was positively affected from PVA and GDC, no statistically significant difference can be attributed to the enhancers. Instead, the pharmacokinetic pattern of 6-cou was highly affected by loading into the lipid matrix: the T_{max} was delayed to 1.5 h for SLN and 3 h for IL and IL PVA, with a more flat absorption peak compared to the free probe. In the case of IL GDC, an early 6-cou absorption peak (45 min after administration) was also detected (Figure 3).

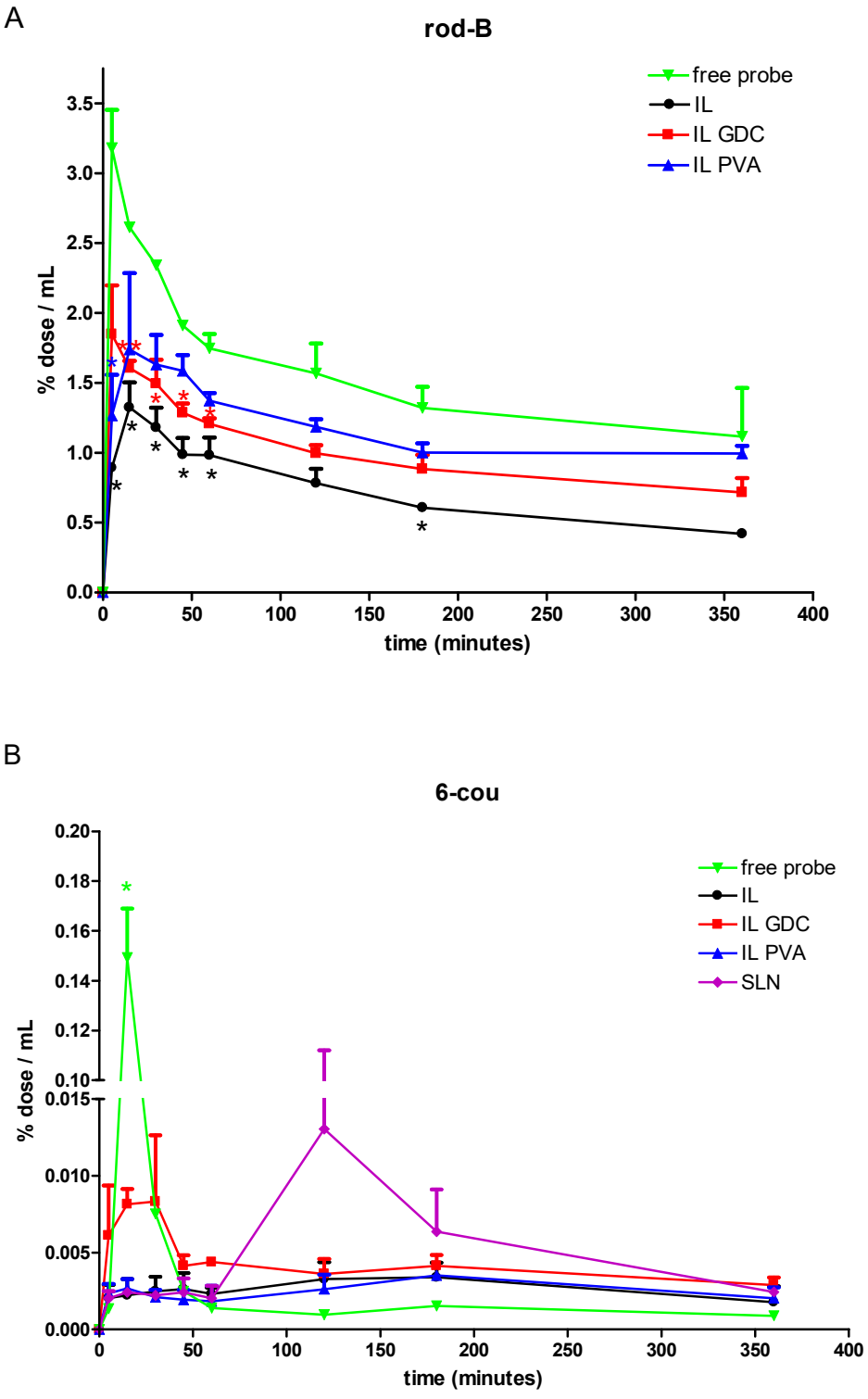

Figure 3. Pharmacokinetics of labelled formulations after intranasal administration to healthy Wistar rats. A) rhodamine B (rod-B) labelled formulations; B) 6-coumarin (6-cou) labelled formulations. Abbreviations: IL: 10% Intralipid®; IL GDC: sodium glycodeoxycholate functionalized IL; IL PVA: 85000-120000 MW 99% hydrolyzed polyvinyl alcohol functionalized IL; SLN: solid lipid nanoparticles. Statistical analysis: A) * IL vs free probe $P<0.05$; * IL GDC vs free probe $P<0.05$; ** IL GDC vs free probe $P<0.01$; * IL PVA vs free probe $P<0.05$ B) * IL, ILGDC, IL PVA, SLN vs free probe $P<0.05$.

Biodistribution studies, shown in Figure 4, were performed by sacrificing the animals at scheduled times nearby the pharmacokinetic T_{max}, with a 30 min lower limit (Table 2) [22,23,25,26]. In the case of 6-cou labelled IL GDC, in separate experiments, animal sacrifices were performed 45 min and 3 h after i.n. administration, in correspondence to 6-cou early and late absorption peak (Figure 4C). For ease of interpretation, in Figure 4B the biodistribution of 6-cou labelled IL GDC obtained after 3 h sacrifice is reported. Comparison between biodistribution after i.v. and i.n. administration of labelled formulations is shown in Figure 5.

Table 2. Timeframe occurring between intranasal administration and animal sacrifice for each formulation under study

Formulation	6-cou	rod-B
SLN	1.5 h	-
IL	3 h	30 min
IL PVA	3 h	30 min
IL GDC	45 min; 3 h	30 min
Free probes	30 min	30 min

Abbreviations: 6-cou: 6-coumarin; IL: 10% Intralipid®; IL GDC: sodium glycodeoxycholate functionalized IL; IL PVA: 85000-120000 MW 99% hydrolyzed polyvinyl alcohol functionalized IL; rod-B: rhodamine B; SLN: solid lipid nanoparticles.

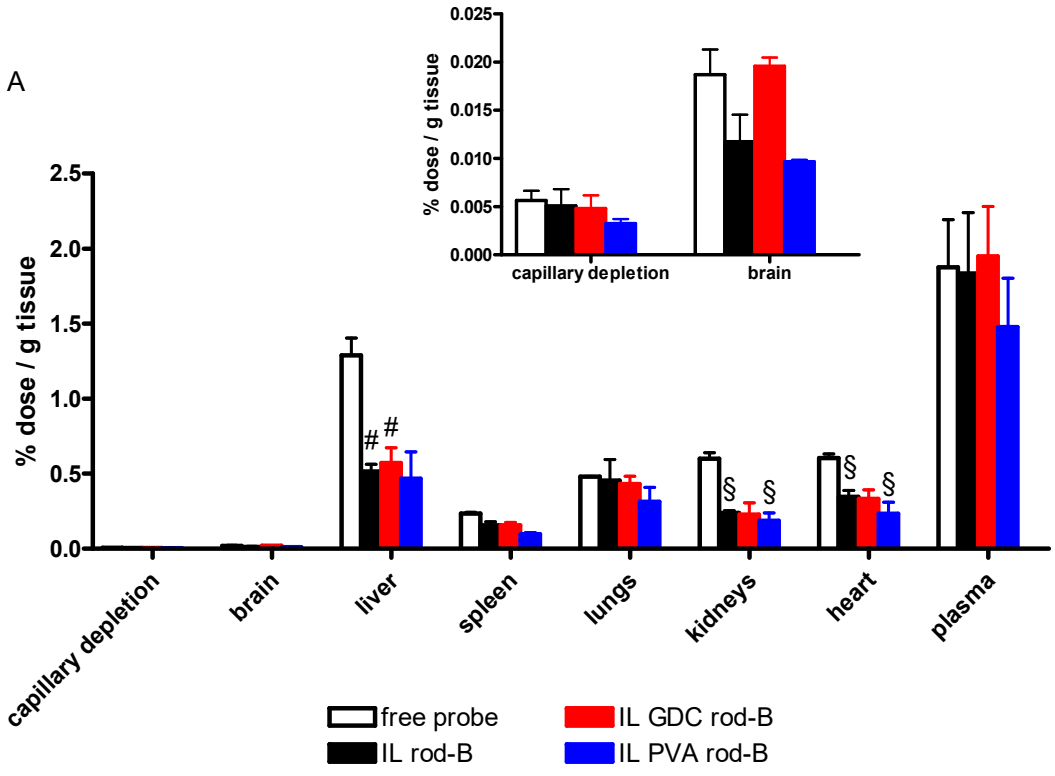

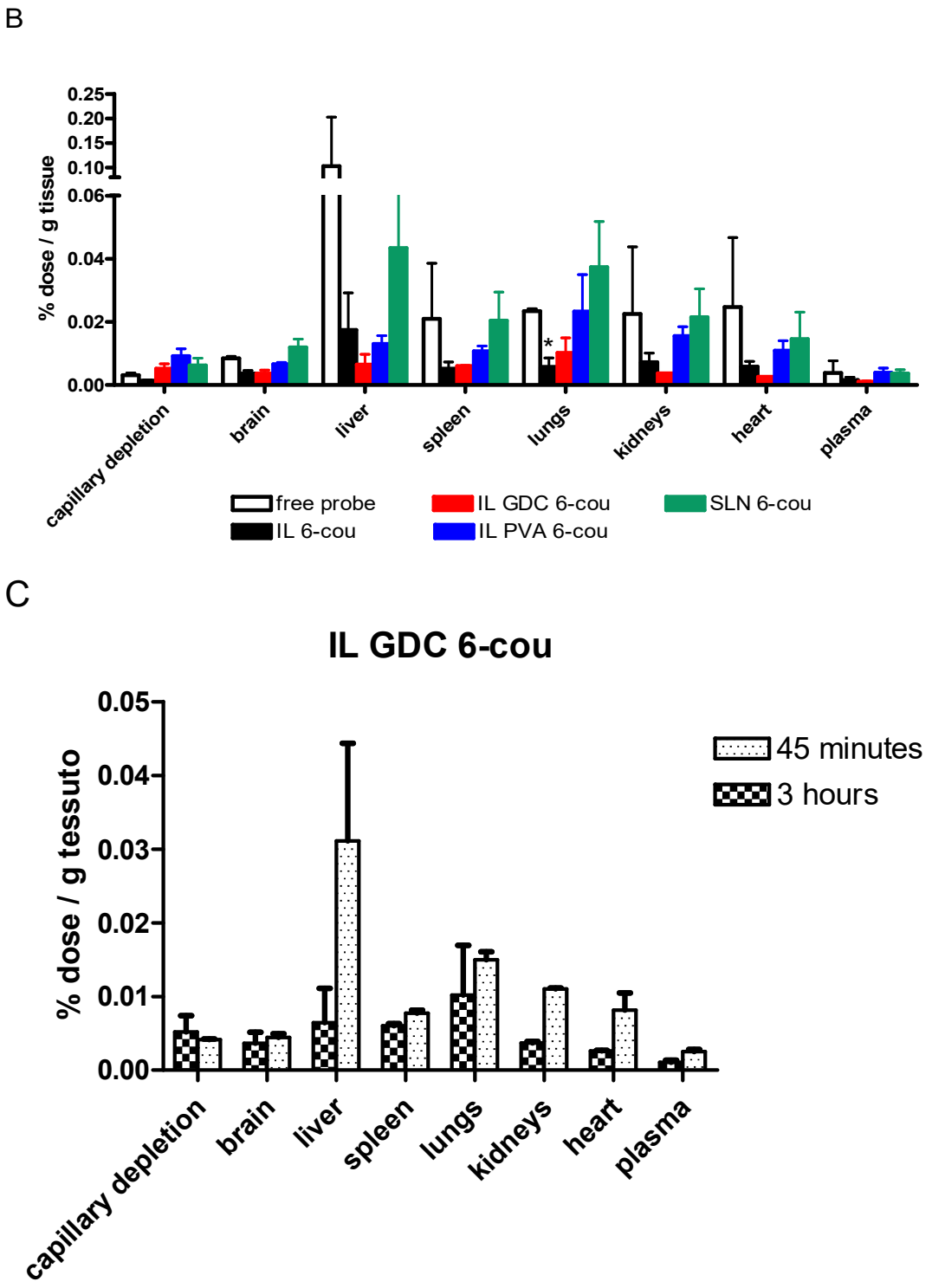

Figure 4. Biodistribution of labelled formulations in healthy Wistar rats after intranasal administration. A) rhodamine B (rod-B) B) 6-coumarin (6-cou) C) 6-cou labelled IL GDC at different time-points after in administration. Abbreviations: IL: 10% Intralipid®; IL GDC: sodium glycodeoxycholate functionalized IL; IL PVA: 85000-120000 MW 99% hydrolyzed polyvinyl alcohol functionalized IL; SLN: solid lipid nanoparticles. Statistical analysis: * free probe vs IL $P<0.05$; # free probe vs IL, IL GDC $P<0.05$; § free probe vs IL, IL PVA $P<0.05$.

A

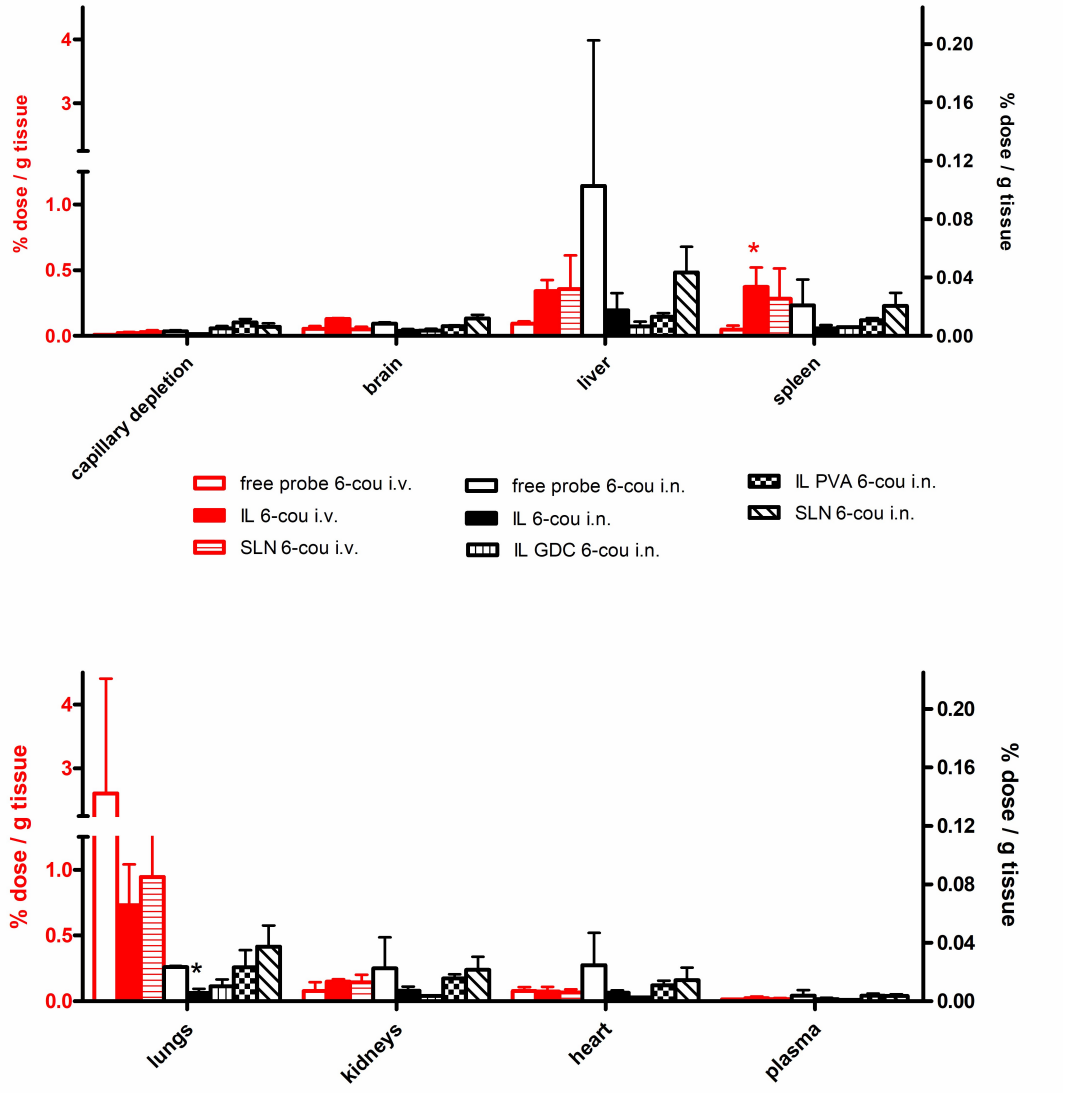
% dose / g tissue
4
3
1.0
0.5
0.0
0.20
0.16
0.12
0.08
0.04
0.00
% dose / g tissue
*
capillary depletion
brain
liver
spleen
free probe 6-cou i.v.
IL 6-cou i.v.
SLN 6-cou i.v.
free probe 6-cou i.n.
IL 6-cou i.n.
IL GDC 6-cou i.n.
IL PVA 6-cou i.n.
SLN 6-cou i.n.
% dose / g tissue
4
3
1.0
0.5
0.0
0.20
0.16
0.12
0.08
0.04
0.00
% dose / g tissue
*
lungs
kidneys
heart
plasma

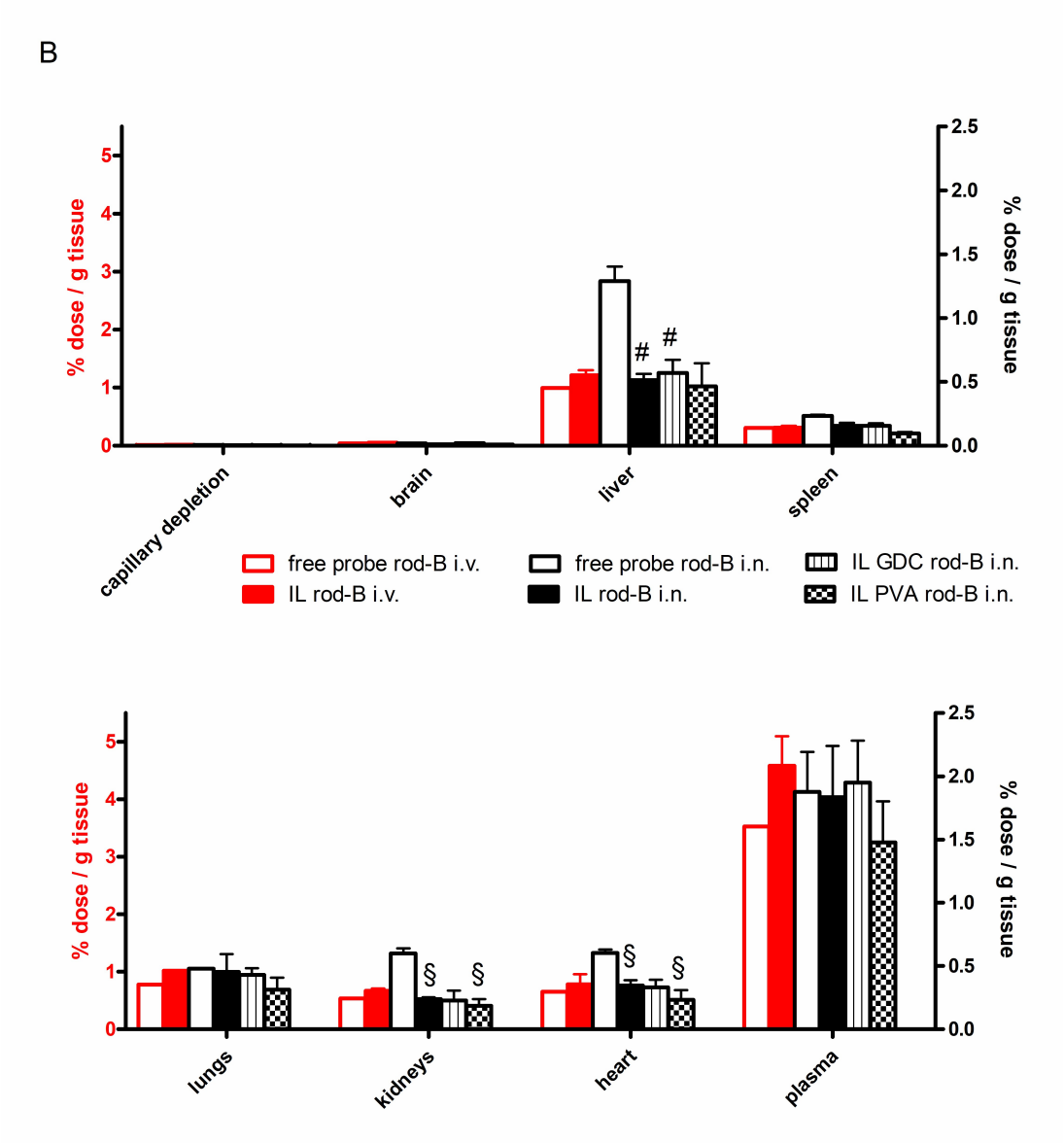

Figure 5. Comparison between biodistribution after intranasal (i.n.) and intravenous (i.v.) administration. A) 6-coumarin (6-cou) labelled formulations B) rhodamine B (rod-B) labelled formulations. Abbreviations: IL: 10% Intralipid®; IL GDC: sodium glycodeoxycholate functionalized IL; IL PVA: 85000-120000 MW 99% hydrolyzed polyvinyl alcohol functionalized IL; SLN: solid lipid nanoparticles. Statistical analysis: * free probe vs IL $P<0.05$; # free probe vs IL, IL GDC $P<0.05$; § free probe vs IL, IL PVA $P<0.05$.

In agreement with permeation and pharmacokinetic studies, a nearly 10 folds higher tissue accumulation was measured for rod-B compared to 6-cou. However, 6-cou distribution into the brain is proportionally more pronounced compared to rod-B. Moreover, for rod-B labelled formulations some considerations can be done: major accumulation organs were similar for the free probe and labelled nanocarriers after i.n. administration. Tissue accumulation after i.n. administration was comparable to that after i.v., used as reference; in some organs, such as liver, heart and kidneys, loading in IL decreases rod-B accumulation, in agreement with the lower nasal permeation and pharmacokinetic profile. Plasma was the main site of accumulation for rod-B, while reticulo-endothelial system (RES) organs [21] were not specifically targeted. 6-cou labelled formulations showed an opposite behavior. Indeed, a nearly 20-folds lower tissue accumulation was measured after i.n. administration compared to i.v. Furthermore, different biodistribution patterns were detected for the labelled formulations under study: there was accumulation in RES organs, but proportionally less pronounced with lipid nanocarriers, whereas liver was the major target tissue for the free

probe. GDC seems to slightly influence 6-cou biodistribution in a time dependent manner (Figure 4C), since the mean initial liver accumulation decreased 3 h after administration.

DISCUSSION

This study aims to predict the hypothetic fate of drug compounds, loaded in two lipid nanocarriers, after i.n. administration, by using two analogous fluorescent probes, based upon their water solubility. Therefore, in preliminary experiments, a wide range of experimental conditions were compared, despite reduced cohorts of animals were employed for each of them. Furthermore, in order to compare such large number of conditions, standardization of the administration protocol was preliminarily established. Indeed, some major concerns are associated with efficient i.n. delivery, one of the most important being the "nasal valve". In fact, the nasal cavity can be divided in 3 different areas: vestibular, olfactory, and respiratory [25]. The vestibular one is the first barrier against airborne particles with low vascularization; the second one enables olfactory perception and is highly vascularized; the last one provides air-cleansing owing to its mucus layer produced by specialized cells [26]. The "nasal valve" is a constriction located between the caudal and the upper cartilage and the septum, whose shape resembles an acute triangle based on the nasal floor in the vestibular zone [2]. It acts as an air resistor, by forcing air stream through a right-angle change, before entering the bone nasal cavity, via the vertical piriform aperture [27]. Therefore, it constitutes the main obstacle for nasal drugs to reach the olfactory and respiratory epithelia. Indeed, nasal devices, such as inhalers that overcome the nasal valve, strongly improve nose-to-brain delivery compared to nasal droplets and sprays [5]. On the other side, frequently i.n. administration in animal models is associated to the employment of anesthesia, especially in the case of large volumes. Nonetheless, parenteral anesthesia affects mucociliary clearance more heavily than inhalation anesthesia, with an alteration of the physiological condition [28]. Therefore, we decided to employ a fractionated i.n. administration of the formulations during a 10 min timeframe, when animals were kept under inhalation anesthesia. In this way, relatively large volumes can be administered, the inhibition of mucociliary clearance is negligible and the airflow associated to inhalation anesthesia can contribute to overcome the nasal valve, approximating the function of an inhaler device.

According to the experimental data obtained, the most striking differences were appreciated between formulations labelled with different probes (6-cou *vs* rod-B), rather than between different nanocarriers (SLN *vs* IL) or among permeation enhancers. Particularly, in Figure 6 an uptake mechanism for labelled IL based formulations is hypothesized. Indeed, rod-B is promptly released from IL formulations: burst release occurs towards the plasma after i.v. administration, and towards the mucus layer after i.n. administration. As a small MW molecule, released rod-B permeates easily and fast the nasal mucosa by paracellular and transcellular route, with good systemic bioavailability, but low selectivity for the brain. Moreover, being promptly dissociated from IL, accumulation in RES organs is not pronounced. Entrapment into IL decreases the probe permeation, probably because of its partitioning into the lipid matrix. On the other side, 6-cou works as a label for the lipid matrix. Therefore, it is associated with delayed permeation and poor systemic bioavailability after i.n. administration, due to the larger size of lipid nanocarriers compared to the free probe. However, a proportionally more pronounced brain accumulation is present compared to rod-B labelled formulations. Given the slow uptake of the 6-cou labelled formulations in the bloodstream, it could be hypothesized that, analogously, slow intraneuronal route plays a role in the nose-to-brain uptake of nanocarriers. The employment of enhancers for IL formulations does not lead to a significant improvement of nasal absorption: the slight increase of the mean pharmacokinetic profile *in vivo* should be confirmed by further studies on larger cohorts of animals, and exceeds the aims of this preliminary study. However, being a surfactant, GDC might cause partial micellization/solubilization of 6-cou at the nasal mucosa, leading to an early pharmacokinetic peak and an initial liver accumulation of the free probe.

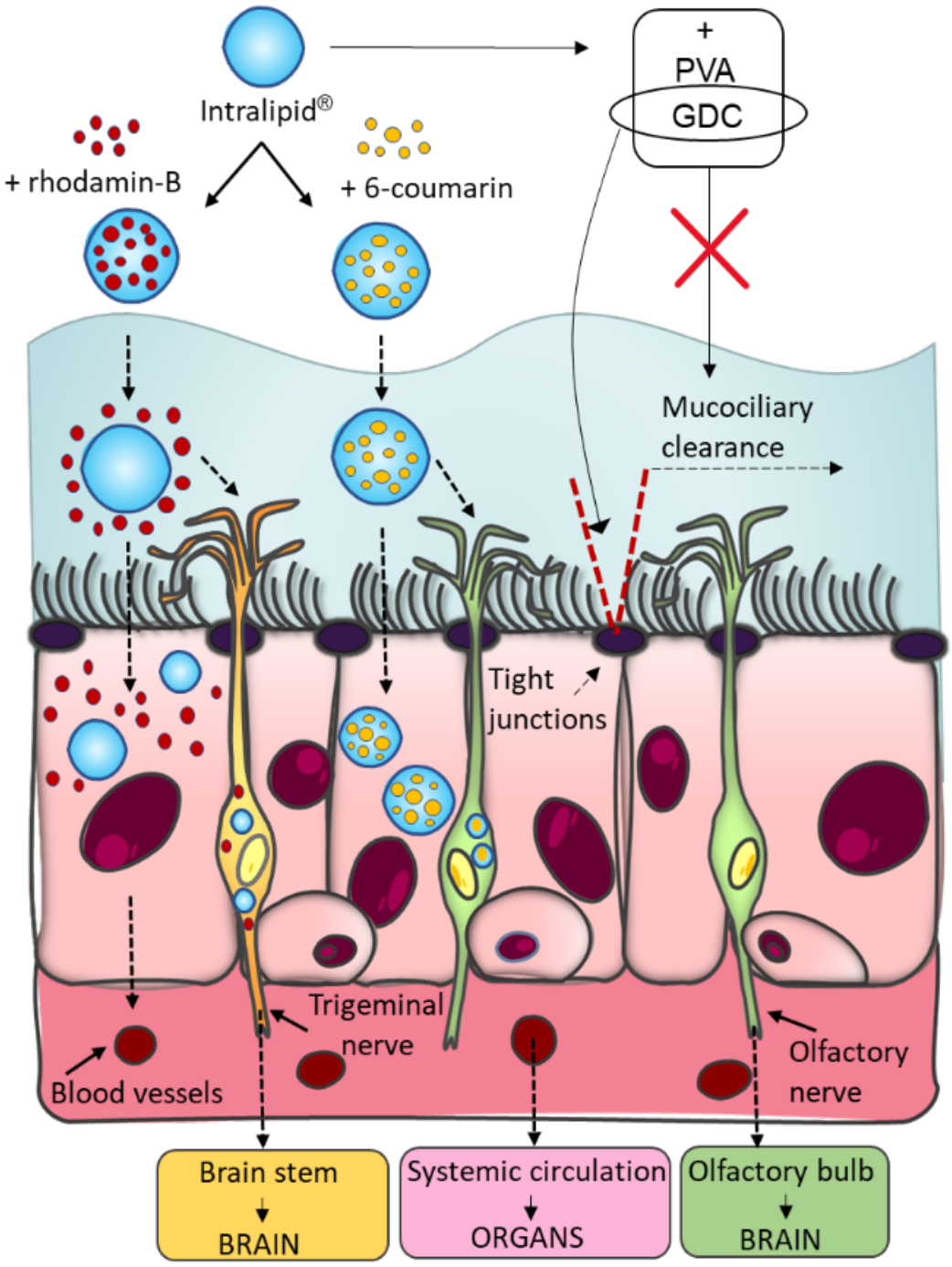

Figure 6. Scheme of probes release and uptake at the nasal mucosa. Abbreviations: GDC: sodium glycodeoxycholate PVA: 85000-120000 MW 99% hydrolyzed polyvinyl alcohol.

At clinical level, intranasal drugs are commonly administered as solutions or powder formulations, which need to undergo a dissolution process before absorption. Indeed, several studies have reported nose-to-brain uptake by simply dissolving drugs in an aqueous phase, which produced significant pharmacological effects [29,30]. Lipophilic drugs easily pass through biomembranes; however, they are poorly water soluble. In contrast, very hydrophilic polar drugs may not have the ability to cross biomembranes [31]. Moreover, although clinical studies have shown a pharmacological response of drugs administered via the nose-to-brain route, preclinical studies reveal that only a small fraction of the administered dose is actually delivered to the brain with conventional nasal solutions, especially for peptide drugs, which are of relevant therapeutic interest [32-35]. The addition of specialized excipients boosts brain

delivery via the nasal route, without causing damage or permanent change to the tissue [36]. In general, the absorption enhancers may act through one of the following mechanisms: tight junctions opening, decreased mucociliary clearance, enzyme activity inhibition, mucus viscosity/elasticity reduction [37,38]. Surfactants are the most effective permeation enhancer, but epithelial toxicity, ciliostatic activity, and nasal irritation are their main drawbacks [39]. Biliary salts were found to be less irritating, to have lower haemolytic activity and less protein release than other surfactants [40]. Gelling agents are used [41], since increasing solution viscosity may prolong the therapeutic effect of nasal preparations. However, increase the viscosity retards diffusion of drug from the matrix and may cause unwanted delay in drug absorption [42]. Thus, to address the low drug delivery problem, scientists are conducting experiments with colloidal systems like nanoemulsions and nanoparticles [43-45]. It is not clear if those formulations increase drug absorption by transporting encapsulated drug across the membrane or just because they enhance the nasal retention time and stability of the drug [46]. Controversial results were found when using nasal nanoparticles. Their low bioavailability can be due to the fact that particles are probably taken up by M-cells in the nasal-associated lymphoid tissue and, therefore, transported into the lymphatic system and bloodstream [47]. On the contrary, it has been found that 100 nm nanoemulsion particles penetrated the olfactory bulb and reached the brain, even to a small extent [48]. Recently, animal studies have shown that nanoemulsions effectively promoted nasal delivery of small molecular weight hydrophobic molecules, such as cyclosporine-A, to the brain without systemic absorption [49]. Moreover, active targeting [50], as well as positively charged nanocarriers [51], exerts a promoting effect on nose-to-brain delivery.

The total extent of nose-to-brain uptake obtained in this experimental study with fluorescently labelled lipid nanocarriers seems lower compared to analogous drug delivery literature studies [52-61]. Nonetheless, many discrepancies are reported among studies at preclinical level, due to the variable experimental protocols employed, and to the different physico-chemical features of nanocarriers and loaded drugs. Therefore, making comparisons among delivery systems is difficult. However, this study clearly shows the influence of water solubility on the behaviour of compounds after i.n. administration, whereas the strength of the association with the lipid matrix likely determines the *in vivo* fate of loaded compounds. Recently, this concern was addressed in a research paper, showing that integral nanoemulsions can be delivered to the olfactory bulb, but few to the brain, whereas the loaded cargoes can be released and permeated into the brain in greater amounts [48]. Nonetheless, no quantification of the phenomenon was performed. Accordingly, our data indicated a limited extent of brain accumulation of 6-cou, which is strongly associated to the lipid matrix, regardless of the nanocarrier employed, while systemic uptake of soluble rod-B is favoured. Probably delivery with intranasal nanocarriers could be optimized by using compounds with intermediate solubility and release properties.

CONCLUSIONS

Several advantages have been hypothesized for i.n. administration of drugs, aiming both to nose-to-brain and systemic absorption. This experimental study investigated the potential of two lipid nanocarriers as drug delivery systems for i.n. route. To this aim, two lipophilic fluorescent probes with different water solubility were employed, in order to mimic the behavior of hypothetic drug compounds. 6-cou, strongly associated to the lipid matrix, was taken up to a limited extent, within a long timeframe, but with a proportionally more pronounced brain accumulation. Rod-B, slightly water soluble, underwent systemic uptake, with good bioavailability, likely due to prompt release at the nasal mucosa. Accordingly, lipid nanocarriers might be optimized for i.n. drug delivery purposes, taking advantage of drug compounds with intermediate solubility and release properties.

Supporting Information: Additional experimental details including:

- Figure S1: cross section of the bovine nasal mucosa lining the turbinates.

Funding: This work was supported by Italian MIUR (FABR 2017), University of Turin (Ricerca Locale 2018-2019) and Fondazione CRT (2021.AI1456.U1618).

REFERENCES

[1] A. Mistry, S. Stolnik, L. Illum, Nanoparticles for direct nose-to-brain delivery of drugs. Int. J. Pharm. 379 (2009) 146–157.

[2] D. Mittal, A. Ali, S. Md, S. Baboota, J.K. Sahni, J. Ali, Insights into direct nose to brain delivery: current status and future perspective. Drug. Deliv. 21 (2014) 75–86.

[3] J.J. Lochhead, R.G. Thorne, Intranasal delivery of biologics to the central nervous system. Adv. Drug. Deliv. Rev. 64 (2012) 614–628.

[4] M.A. Lauzon, A. Daviaua, B. Marcos, N. Faucheux, Nanoparticle-mediated growth factor delivery systems: a new way to treat Alzheimer's disease. J. Control. Rel. 206 (2015) 187–205.

[5] P.G. Djupesland, J.C. Messina, R.A. Mahmoud, The nasal approach to delivering treatment for brain diseases: an anatomic, physiologic, and delivery technology overview. Ther. Del. 5 (2014) 709-733.

[6] M. Shadab, M. Gulam, B. Sanjula, A. Javed, Nanoneurotherapeutics approach intended for direct nose to brain delivery. Drug. Dev. Ind. Pharm. 41 (2015) 1922–34.

[7] S. Sood, K. Jain, K. Gowthamarajan, Intranasal therapeutic strategies for management of Alzheimer's disease. J. Drug. Target. 22 (2014) 279–294.

[8] L. Illum, Nasal drug delivery: new developments and strategies. Drug. Discov. Today. 7 (2002) 1184–1189.

[9] L. Illum, Nasal drug delivery – recent developments and future prospects. J. Control. Rel. 161 (2012) 254–263.

[10] L. Battaglia, P.P. Panciani, E. Muntoni, M.T. Capucchio, E. Biasibetti, P. De Bonis, S. Mioletti, M. Fontanella, S. Swaminathan, Lipid nanoparticles for intranasal administration: application to nose-to-brain delivery. Expert. Opin. Drug Deliv. 15(4) (2018) 369-378.

[11] Y. Huang and M.D. Donovan. Large molecule and particulate uptake in the nasal cavity: the effect of size on nasal absorption. Adv. Drug. Deliv. Rev. 29(1-2) (1998) 147-155.

[12] S.S. Hong, K.T. Oh, H.G. Choi & S.J. Lim. Liposomal Formulations for Nose-to-Brain Delivery: Recent Advances and Future Perspectives. Pharmaceutics 11(10) (2019) 540.

[13] A. Sharma, U.S. Sharma. Liposomes in drug delivery: progress and limitations. Int J Pharm 154 (1997) 123-140.

[14] L. Battaglia, M. Gallarate, Lipid nanoparticles: state of the art, new preparation methods and challenges in drug delivery. Expert. Opin. Drug Deliv. 9 (2012) 497–508.

[15] C.P. Costa, J.N. Moreira, J.M. Sousa Lobo, A.C. Silva. Intranasal delivery of nanostructured lipid carriers, solid lipid nanoparticles and nanoemulsions: A current overview of in vivo studies. Acta Pharm. Sin. B 11(4) (2021) 925-940.

[16] J. Patel, Intranasal route for CNS delivery: overview and recent advancements. Eur. J. Pharm. Me. Res. 4(06) (2017) 281-292.

[17] J.H. Finke, C. Richter, T. Gothsch, A. Kwade, S. Büttgenbach, C.C. Müller-Goymann, Coumarin 6 as a fluorescent model drug: How to identify properties of lipid colloidal drug delivery systems via fluorescence spectroscopy? Eur. J. Lipid Sci. Technol. 116 (2014) 1234–1246.

[18] S. Pretor, J. Bartels, T. Lorenz, K. Dahl, J.H. Finke, G. Peterat, R. Krull, A.T. Al-Halhouli, A. Dietzel, S. Büttgenbach, S. Behrends, S. Reichl, C.C. Müller-Goymann, Cellular Uptake of Coumarin-6 under Microfluidic Conditions into HCE-T Cells from Nanoscale Formulations. Mol. Pharmaceutics. 12 (2015) 34–45.

[19] L. Battaglia, M. Gallarate, R. Cavalli, M. Trotta, Solid lipid nanoparticles produced through a coacervation method. J. Microencapsul. 27 (2010) 78–85.

[20] N. Clemente, B. Ferrara, C.L. Gigliotti, E. Boggio, M.T. Capucchio, E. Biasibetti, D. Schiffer, M. Mellai, L. Annovazzi, L. Cangemi, E. Muntoni, G. Miglio, U. Dianzani, L. Battaglia, C. Dianzani, Solid Lipid

Nanoparticles Carrying Temozolomide for Melanoma Treatment. Preliminary In Vitro and In Vivo Studies. Int. J. Mol. Sci. 19 (2018) 255.
[21] E. Muntoni, K. Martina, E. Marini, M. Giorgis, L. Lazzarato, I.C. Salaroglio, C. Riganti, M. Lanotte, L. Battaglia, Methotrexate-Loaded Solid Lipid Nanoparticles: Protein Functionalization to Improve Brain Biodistribution. Pharmaceutics 11 (2019) 65.
[22] D. Triguero, J.B. Buciak, J. Yang, W.M. Pardridge, Blood-brain-barrier transport of cationized immunoglobin G. Enhanced delivery compared to native protein. Proc. Natl. Acad. Sci. USA 86 (1989) 4761–4765.
[23] E. Muntoni, E. Marini, N. Ahmadi, P. Milla, C. Ghè, A. Bargoni, M.T. Capucchio, E. Biasibetti, L. Battaglia, Lipid nanoparticles as vehicles for oral delivery of insulin and insulin analogs: preliminary ex vivo and in vivo studies. Acta-Diabetol. 56 (2019) 1283–1292.
[24] S. Neervannan. Preclinical formulations for discovery and toxicology: physicochemical challenges. Expert Opin Drug Metab Toxicol. 2(5) (2006) 715-31.
[25] C. Bitter, K.S. Zimmermann, C. Surber, Nasal Drug Delivery in Humans. Curr. Probl. Dermatol. 40(c) (2011) 20-35.
[26] A. Pires, A. Fortuna, G. Alves, A. Falcao, Intranasal drug delivery: how, why and what for? J. Pharm. Pharm. Sci. 12 (2009) 288– 311.
[27] P. Cole, The four components of the nasal valve. Am. J. Rhin. 17(2) (2003), 107-110.
[28] S.H. Mayor, L. Illum, Investigation of the effects of anesthesia on nasal absorption of insulin in rats. Int. J. Pharm. 149 (1997) 123-129.
[29] S.U. Islam, A. Shehzad, M.B. Ahmed, Y.S. Lee, Intranasal Delivery of Nanoformulations : A Potential Way of Treatment for Neurological Disorders. Molecules 25 (2020) 1929.
[30] Z. Jassim, E. Jasim, A review on strategies for improving nasal drug delivery systems. Drug Invention Today. 10 (2018) 2857-2864.
[31] Kushwaha, S.K.; Keshari, R.K.; Rai, A. Advances in nasal trans-mucosal drug delivery. J Appl Pharm Sci 1 (2011) 21-28.
[32] S. Craft, L.D. Baker, T.J. Montine, S. Minoshima, G.S. Watson, A. Claxton, M. Arbuckle, M. Callaghan, E. Tsai, S.R. Plymate, Intranasal insulin therapy for Alzheimer disease and amnestic mild cognitive impairment: A pilot clinical trial. Arch. Neurol. 69 (2012) 29–38.
[33] R. Thorne, L. Hanson, T. Ross, D. Tung, W. Frey Ii, Delivery of interferon-beta to the monkey nervous system following intranasal administration. Neuroscience 152 (2008) 785–797.
[34] J. Born, T. Lange, W. Kern, G.P. McGregor, U. Bickel, H.L. Fehm, Sniffing neuropeptides: A transnasal approach to the human brain. Nat. Neurosci. 5 (2002) 514.
[35] K.J. Parker, O. Oztan, R.A. Libove, R.D. Sumiyoshi, L.P. Jackson, D.S. Karhson, J.E. Summers, K.E. Hinman, K.S. Motonaga, J.M. Phillips, Intranasal oxytocin treatment for social deficits and biomarkers of response in children with autism. Proc. Natl. Acad. Sci. USA 114 (2017) 8119–8124.
[36] J. Mundlia, M. Kumar, Nasal drug delivery-an overview. Int J Pharm Sci Res 6 (2015) 951-960.
[37] S. Upadhyay, A. Parikh, P. Joshi, U. Upadhyay, N. Chotai, Intranasal drug delivery system-A glimpse to become maestro. J Appl Pharm Sci 1 (2011) 34-44.
[38] A.K. Singh, A. Singh, N. Madhv, Nasal cavity, a promising transmucosal platform for drug delivery and research approaches from nasal to brain targetting. J Drug Deliv Ther 2 (2012) 22-33.
[39] P.A. Mistri, D. Patel, J.J. Prajapati, Intranasal drug delivery system: A review. Int J Pharm Innov 2 (2012) 88-111
[40] E. Moghimipour, A. Ameri, S. Handali, Absorption-enhancing effects of bile salts. Molecules 20 (2015) 14451-73.
[41] T. Garg, G. Rath, A.K. Goyal, Comprehensive review on additives of topical dosage forms for drug delivery. Drug Deliv 22 (2015) 969-87.
[42] D. Bhowmik, R. Kharel, J. Jaiswal, C. Biswajit, K. Kumar, Innovative approaches for nasal drug delivery system and its challenges and opportunities. Sch Res Lib Ann Bio Res 1 (2010) 21-26.
[43] L. Godfrey, A. Iannitelli, N.L. Garrett, J. Moger, I. Imbert, T. King, F. Porreca, R. Soundararajan, A. Lalatsa, A.G. Schätzlein, Nanoparticulate peptide delivery exclusively to the brain produces tolerance free analgesia. J. Control. Release 270 (2018) 135–144.

[44] Z. Patel, B. Patel, S. Patel, C. Pardeshi, Nose to Brain Targeted Drug Delivery bypassing the Blood-Brain Barrier: An overview. Drug Invent. Today 4 (2012) 610–615.
[45] R. Jayaraj, V. Chandramohan, E. Namasivayam, Nanomedicine for Parkinson disease: Current status and future perspective. Int. J. Pharm. Bio. Sci 4 (2013) 692-704.
[46] S.P. Tated, A.S. Kulkarni, Intranasal Drug Delivery: An Approach for Brain Targeting. The Bomb Tech 59 (2009) 58-66.
[47] G. Buvaneswari, A. Rajalakshmi, Emerging trends in novel drug delivery system. Int Nas Drug Deliv 5 (2016) 67-111.
[48] E. Ahmad, Y. Feng, J. Qi, W. Fan, Y. Ma, H. He, F. Xia, X. Dong, W. Zhao, Y. Lu, Evidence of nose-to-brain delivery of nanoemulsions: Cargoes but not vehicles. Nanoscale 9 (2017) 1174–1183.
[49] S. Yadav, F. Gattacceca, R. Panicucci, M.M. Amiji, Comparative biodistribution and pharmacokinetic analysis of cyclosporine-A in the brain upon intranasal or intravenous administration in an oil-in-water nanoemulsion formulation. Mol Pharm 12 (2015) 1523-33.
[50] L. Wang, X. Zhao, J. Du, M. Liu, J. Feng, K. Hu, Improved brain delivery of pueraria flavones via intranasal administration of borneol-modified solid lipid nanoparticles. Nanomedicine 14(16) (2019) 2105-2119.
[51] M.C. Bonferoni, S. Rossi, G. Sandri, F. Ferrari, E. Gavini, G. Rassu, P. Giunchedi, Nanoemulsions for "Nose-to-Brain" Drug Delivery. Pharmaceutics 11 (2019) 84.
[52] A. Shobo, A. Pamreddy, H.G. Kruger, M.M. Makatini, T. Naicker, T. Govender, S. Baijnath, Enhanced brain penetration of pretomanid by intranasal administration of an oil-in-water nanoemulsion. Nanomedicine 13(9) (2018), 997-1008.
[53] E. Muntimadugu, R. Dhommati, A. Jain, V.G. Challa, M. Shaheen, W. Khan, Intranasal delivery of nanoparticle encapsulated tarenflurbil: A potential brain targeting strategy for Alzheimer's disease. Eur. J. Pharm. Sci. 92 (2016) 224-34.
[54] A.P. Singh, S.K. Saraf, S.A. Saraf, SLN approach for nose-to-brain delivery of alprazolam. Drug Deliv. Transl. Res. 2 (2012) 498–507.
[55] S. Patel, S. Chavhan, H. Soni, A.K. Babbar, R. Mathur, A.K. Mishra, K. Sawant, Brain targeting of risperidone-loaded solid lipid nanoparticles by intranasal route. J Drug Target 19(6) (2011) 468-474.
[56] K.T. Ko, T.E. Needham, H. Zia, Emulsion formulations of testosterone for nasal administration. J. Microencapsul. 15(2) (1998) 197-205.
[57] E.M. Abdou, S.M. Kandil, H.M.F.E. Miniawy, Brain targeting efficiency of antimigrain drug loaded mucoadhesive intranasal nanoemulsion. Int. J. Pharm. 529(1-2) (2017) 667-677.
[58] S. Eskandari, J. Varshosaz, M. Minaiyan, M. Tabbakhian, Brain delivery of valproic acid via intranasal administration of nanostructured lipid carriers: in vivo pharmacodynamic studies using rat electroshock model. Int. J. Nanomedicine. 6 (2011) 363-371.
[59] M. Kumar, V. Kakkar, A.K. Mishra, K. Chuttani, I.P. Kaur, Intranasal delivery of streptomycin sulfate (STRS) loaded solid lipid nanoparticles to brain and blood. Int. J. Pharm. 461(1-2) (2014) 223-233.
[60] H.M. Aboud, M.H. El komy, A.A. Ali, S.F. El Menshawe, A.A. Elbary, Development, Optimization, and Evaluation of Carvedilol-Loaded Solid Lipid Nanoparticles for Intranasal Drug Delivery. AAPS Pharm. Sci. Tech. 17 (2016) 1353–1365.
[61] H.S. Mahajan, M.S. Mahajan, P.P. Nerkar, Nanoemulsion-based intranasal drug delivery system of saquinavir mesylate for brain targeting. Drug. Deliv. 21(2) (2014) 148-154.